8/1/80

LBL-10843
Preprint

c.2

Lawrence Berkeley Laboratory
UNIVERSITY OF CALIFORNIA

Accelerator & Fusion Research Division

RECEIVED
AUG 01
LIBRARY
DOCUMENTS

Submitted to Physical Review B

H^- and D^- PRODUCTION BY BACKSCATTERING FROM ALKALI-METAL TARGETS

P. J. Schneider, K. H. Berkner, W. G. Graham,
R. V. Pyle, and J. W. Stearns

July 1980

TWO-WEEK LOAN COPY

This is a Library Circulating Copy which may be borrowed for two weeks. For a personal retention copy, call Tech. Info. Division, Ext. 6782

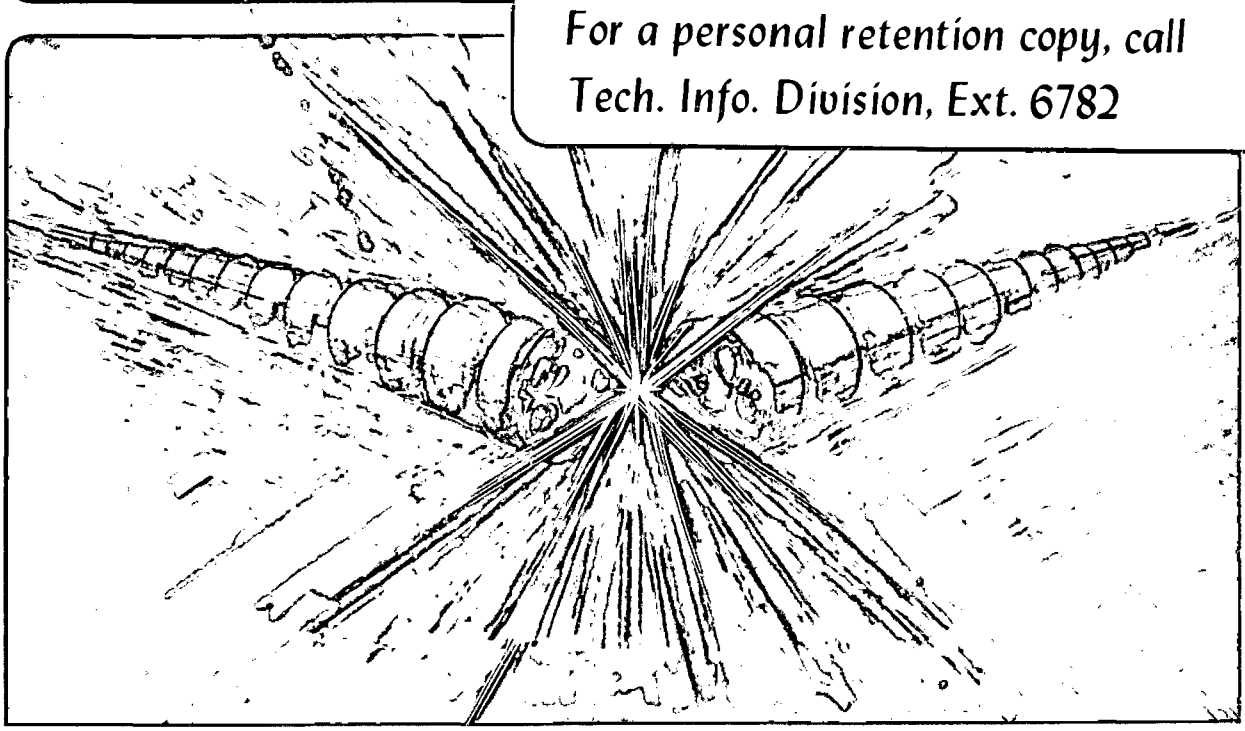

Prepared for the U.S. Department of Energy under Contract W-7405-ENG-48

LBL-10843 c.2

DISCLAIMER

This document was prepared as an account of work sponsored by the United States Government. While this document is believed to contain correct information, neither the United States Government nor any agency thereof, nor the Regents of the University of California, nor any of their employees, makes any warranty, express or implied, or assumes any legal responsibility for the accuracy, completeness, or usefulness of any information, apparatus, product, or process disclosed, or represents that its use would not infringe privately owned rights. Reference herein to any specific commercial product, process, or service by its trade name, trademark, manufacturer, or otherwise, does not necessarily constitute or imply its endorsement, recommendation, or favoring by the United States Government or any agency thereof, or the Regents of the University of California. The views and opinions of authors expressed herein do not necessarily state or reflect those of the United States Government or any agency thereof or the Regents of the University of California.

Submitted to Phys. Rev. B. LBL-10843

H^- and D^- Production by Backscattering from Alkali-Metal Targets*

P. J. Schneider[+], K. H. Berkner, W. G. Graham[++], R. V. Pyle and J. W. Stearns

Lawrence Berkeley Laboratory, Univ. of Calif. Berkeley, Ca. 94720

ABSTRACT

Measurements have been made of the total baskscattered D^- and H^- yields from thick, clean targets of Cs, Rb, K, Na and Li, bombarded with H_2^+, H_3^+, D_2^+, D_3^+ with incident energies from 0.15 to 4.0 keV/nucleus. All of the measurements were made at background pressures less than 10^{-9} Torr, and the alkali-metal targets were evaporated onto a cold substrate (T $\sim$77K) in situ to assure thick, uncontaminated targets. For each target, the H^- and D^- yields exhibited maxima (as high as 0.08 per incident proton or deuteron) at incident energies between 0.3 and 1.4 keV/nucleus. For both hydrogen and deuterium incident at any energy, the negative ion yield decreases in going from Cs to Li in the other given above. Also, a definite isotope effect was observed for every target used, with the H^- yield peaking at a lower incident energy than the D^- yield and in most cases, the maximum H^- yield was higher than the maximum D^- yield. Measurements of the D^- yield as a function of Cs coverage were also made for D_3^+ bombarding a Ni substrate. The D^- yield maximized at or near the coverage at which the surface work function reached a minimum.

* Work supported by U. S. Department of Energy, Office of Fusion Energy under contract W-7405-ENG-48.

[+]Present address: Max Planck Institute for Plasmaphysics, Garching, West Germany.

[++]Present address: The New University of Ulster, Coleraine, Northern Ireland.

Introduction

Recent experiments have shown that it is possible to dramatically increase negative-ion yields from ion sources by adding an alkali metal to the discharge.[1,2] In H^- sources, the addition of Cs to the discharge has resulted in increases of more than an order of magnitude in the H^- current density.[3] Belchenko, Dimov and Dudnikov[3,4,5] and Hiskes, Karo and Gardner[6] have proposed models based upon surface production as the principal mechanism for H^- formation in these sources. Belchenko, Dimov and Dudnikov proposed that any hydrogen atom adsorbed on the surface has a high probability of residing as a negative ion and can be desorbed from the surface as a negative ion by an incident energetic particle from the discharge. The addition of Cs to the H^- source produces Cs coverage of the source surfaces; this lowers the surface work function, enhances the probability of escape without destruction of the negative ion from the surface, and increases the H^- yield. Hiskes, Karo and Gardner have hypothesized that H^- ions are formed in the collision of an energetic (1 to 100 eV) hydrogen atom with an adsorbed Cs atom. The H^- formation process takes place via the CsH, CsH^- molecular potentials: As the hydrogen atom approaches the adsorbed Cs atom the interaction potential is taken to be the difference between the image potential and the CsH^- electron affinity. This potential allows the resonant transfer of an electron from the substrate to the hydrogen atom, which in turn may escape from the surface as H^-.

H^- production from surfaces involves three processes: The reflection or desorption of the hydrogen from the surface, the formation of the negative ion at the surface, and the escape-without-destruction of

the negative ion from the surface. In the mechanism proposed by Belchenko, Dimov and Dudnikov,[3,4,5] the probability of formation of the negative ion is unity and the probabilities of desorption and escape-without-destruction become the dominant factors in determining the negative-ion yield from the surface. In the partial-coverage model of Hiskes and Karo,[7] the probability of destruction of the negative ion is shown to be negligible, so that the probability of formation of the negative ion, along with the probability of reflection of the incident particle, become the dominant factors in determining the negative-ion yield from the surface.

These models have led to calculations of the H^- secondary emission coefficient (the number of negative ions emitted from the surface per incident nucleus) by Kishinevskii[8] and Hiskes and Karo[7]. Kishinevskii has estimated the H^- secondary emission coefficient to be 0.1 to 0.2 for particles leaving the surface with energies of tens of eV. Hiskes and Karo have calculatd both formation and escape probabilities for surfaces with a partial monolayer coverage of Cs. They have combined their results with those of Oen and Robinson[9], who have used a Monte-Carlo technique to calculate the reflected fraction of the incident particles as a function of incident energy, to predict H^- secondary emission coefficients of 0.5 to 0.3 over the backscattered-energy range 10 to 100 eV. Hiskes and Karo[7] have also calculated the escape probabilities from some thick alkali-metal surfaces.

There exist almost no experimental measurements for comparison with the above calculations. Therefore, we have measured the total backscattered H^- and D^- yields from various alkali-metal surfaces.

The experiment was divided into two parts: (1) clean, thick, alkali-metal targets (Cs, Rb, K, Na, and Li) and (2) thin coverage of Cs on a Ni substrate. For the thick targets, the incident energy of the hydrogen and deuterium ions ranged from 0.15- to 4 keV/nucleus and for the thin-coverage targets the range was from 0.4- to 0.9 keV/nucleus.

For reasons discussed in the next section it was necessary to use molecular ions: D_2^+, D_3^+, H_2^+ and H_3^+. At the energies used here, molecular ions at normal incidence are dissociated at the surface,[10,11] hence the D^- and H^- yields were normalized to the number of nucleii per incident ion to obtain D^- per incident deuteron or H^- per incident proton. The D_3^+ and H_3^+ ions were used to obtain the lowest incident velocities, due to the limit imposed by low-energy beam transport to the target. The D_2^+ and H_2^+ ions were used to verify that the negative ion yields were indeed independent of the number of nucleii per incident molecular ion.

By varying the energy of the incident ions, the work function and the mass of the target, we have attempted to determine which parameters are important to the conversion of incident particles to backscattered negative ions and how these parameters may be varied to optimize the negative ion yield.

Apparatus and Procedure

A beam of D_2^+ (H_2^+) and D_3^+ (H_3^+) ions was extracted from a hot-filament discharge, accelerated to the desired energy, and momentum selected with a 30° bending magnet before entering the experimental chamber, which is described in greater detail in reference 12. The

apparatus within the chamber (Figure 1) was designed around two rectangular plates, perpendicular to the beam line; an aperture in the first plate (the collector) allowed the beam to pass through to the second plate (the target) from which D^- (H^-), D^0 (H^0), D^+ (H^+), e^- as well as sputtered particles were emitted. The collector was used to monitor the negative-ion current, therefore, all other charged particles had to be prevented from reaching or leaving it: An electric field between the target and collector plates prevented positive secondary ions from reaching the collector and a transverse magnetic field suppressed secondary electrons. Also, an upbeam collimator shielded the collector from the primary beam. This collimator was the endplate of a Faraday cup (the collimator-Faraday cups) which was used to determine the total current incident onto the target: The total incident current was determined by the difference in current readings from the collimator-Faraday cup when the beam was deflected into the cup and when it was steered through the cup by a pair of upbeam deflection plates. The negative ion secondary emission coefficient (NISEC) was determined by taking the ratio of the collector current to the total incident current and dividing by the number of deuterons (protons) per incident molecular ion.

The collimator-Faraday cup, which was 2.5 cm in diameter, 4 cm long and had a 0.15-cm-diam exit aperture, was 0.08 cm upbeam from the collector.

The electric field used to suppress positive ions was produced by applying a negative voltage to the target. The magnitude of the applied voltage was determined by the beam specie and energy. As an example, a

5.0-keV beam of D_3^+ required a target bias of at least -2.5 kV. The target bias adds to the incident energy giving a total incident energy of 7.5 keV; if we assume that the energy is divided equally between the three deuterons as the incident ion breaks up at the surface, then the maximum energy that a reflected D^+ ion can have is less than 2.5 keV, which is not sufficient for it to reach the collector plate. This explains why, in this experiment, D^+ and H^+ were not used as incident particles. For D^+ the maximum reflected energy is always greater than the retarding voltage, so that the high-energy backscattered D^+ ions cannot be prevented from reaching the collector.

The transverse magnetic field used to suppress secondary electrons from the target, the collector and the collimator-Faraday cup was produced by an electro-magnet with a 6.5-cm gap and 5-cm-diam poles. The suppression of secondary electrons is illustrated in Fig. 2, where the "apparent" NISEC is plotted vs the magnitude of the magnetic field. At low magnetic fields the signal is dominated by electrons, which are suppressed as the magnetic field is increased. For the case illustrated in Fig. 2 (3 keV/nucleon D_3^+, $|E_{gap}|$ = 4.6 kV/cm) 650 gauss is sufficient for complete electron suppression. Calculations of trajectories for D^- ions emitted from the target show that all negative ions (even those emitted with zero energy) reach the collector for all electric and magnetic fields used in this experiment.

The target and collector plates were 7.3-cm high, 5-cm wide, and separated by 1.3 cm; the collector-plate aperture was 0.25 cm in diameter. To assure that all the negative ions produced at the target were collected, two separate tests were performed. The first test was to

vary the effective width of the collector plate with a series of electrically isolated masks. The currents collected by the masks and by the collector were measured as a function of collector width. The ratio of the collector current to the sum of these currents remained constant at 0.99 for collector widths down to 3.6 cm and decreased as the collector width was further decreased. The second test was to vary the effective diameter of the aperture in the collector plate from 0.25 cm to 0.7 cm with another series of electrically isolated masks which covered the collector plate. The ratio of the current on the mask to the current on the collector behind it was measured as a function of the diameter of the aperture. Extrapolation to zero diameter indicated that the loss of negative ions through the 0.25-cm-diameter aperture was (5 $\pm$ 5)%. From these tests, which were performed for incident energies from 0.75 to 3 keV/nucleon and with various electric and magnetic fields, we concluded that the dimensions of the collector plate were large enough, and the aperture small enough, to ensure that (95 $\pm$ 5)% of the negative ions were collected.

Positive ions produced by backscattered particles (atoms and negative ions) striking the collector could not be suppressed. The current due to these ions leaving the collector adds to the current from the collected negative ions and is a possible source of error. To investigate the magnitude of this effect, the NISEC was measured for a sodium target, with a stainless steel collector. Then the target was heated to evaporate the sodium onto the collector. The dispensor was used to re-coat the target with sodium and the NISEC measurement was repeated. Changing the collector surface from stainless steel to sodium

changes the collector work function from 4 eV to 2.3 eV and greatly changes the charge distribution of the backscattered particles leaving the collector (very few positive ions leave the sodium surface). No difference was seen in the NISEC measurements using the two collector surfaces.

Meishnev and Verbeek[13] and Eckstein et al.[14] have measured the ratio of protons to neutrals emerging from various metal targets as a function of exit energy and angle. Their results indicate that for an exit energy of 1 keV, less than 5% of the merging particles are positive ions, with the positive ion fraction dropping off rapidly at lower energies. These results, along with the measurements using the two collector surfaces, led to the conclusion that the effect of positive ions leaving the collector was less than the differences in reproducibility of the experimental measurements (5%).

Clean alkali-metal targets were deposited on a liquid-nitrogen-cooled substrate in the cryopumped experimental chamber, which was maintained at a pressure less than 10^{-9} Torr during the measurements. An S.A.E.S.* alkali-metal dispenser, mounted on a bellows, could be positioned between the target and collector plates to coat the target area. The thickness of the alkali-metal layer was controlled by varying the current through the dispenser (6 to 8A) and the evaporation time. As an example, from the manufacturer's data we estimate that passing 7.5A through a Na dispenser for three minutes results in a Na layer about 15?m

---

*SAES Getters/USA, Crystal Springs, Colorado.

thick (assuming a Na sticking coefficient of unity), which is the same order of magnitude as the average penetration depth of a 1-keV deuteron.[15]

Surface purity was monitored by mass-analysis of positive ions sputtered from the surface by an 8 keV Ar^+ beam. An electrostatic-quadrupole mass analyzer, was placed in the chamber so that it sampled ions leaving the surface at an angle of 50° to the surface normal.[12] Prior to evaporation, many different mass peaks were observed, indicating extensive surface contamination (Figure 3A); after a thick alkali-metal target was deposited, the positive-ion spectrum showed only peaks corresponding to sputtered alkali-metal target ions (Figure 3B). To determine if the sputtered impurity ions contributed significantly to the total negative ion signal, incident beams of Ar^+ at 8 keV were used. The results showed that the sputtered negative ions (either H^- or impurities) contributed less than 5% of the total negative signal on the collector; hence within our experimental estimated uncertainty of 10%, the NISEC measured in this experiment is the backscattered H^- yield.

For H^- yield measurements from thin coverage of a substrate, changes in the surface work function were measured using the retarding potential method.[15,16,17,18] A hot tungsten filament could be positioned directly in front of the target, and by measuring the shift in the I-V curves of the diode formed by the filament and the target, the change in the target work function relative to that of the filament was obtained.[12]

Results and Discussion

A. Thick-coverage

Figures 4 to 13 show the measured values of the backscattered D^- and H^- yields for Cs, Rb, K, Na and Li targets as a function of the energy of the incident ions. The estimated standard uncertainties ($\pm$ 10%) indicated in the figures are the result of considering the effects discussed in the text (losses through the collector aperture and positive ions leaving the collector) as well as the calibration of the electrometers and reproducibility of the measurements.

There are some features worth noting in Figs. 4 through 13

(1) Each target shows a maximum in the H^- and D^- yields.

(2) The maximum value of the $H^-(D^-)$ yield decreases in the order Cs, Rb, K, Na and Li at any incident energy.

(3) The higher the maximum value of the $H^-(D^-)$ yiled, the lower the incident energy at which it occurs.

(4) For any given target the maximum in the D^- yield is less than or equal to the maximum in the H^- yield and occurs at a higher incident energy than the H^- maximum.

(5) The H^- yield per incident proton is the same for H_2^+ and H_3^+ ions incident, and the D^- yield per incident deuteron is the same for D_2^+ and D_3^+ incident, but, at a given incident energy, the D^- and H^- yields are not equal.

The results of these measurements can be interpreted by considering the H^- yield as a function of the probability of reflection of the incident particles, $n(\vec{v})/N_i$, the probability of formation of the H^- ion at the target $P_-(\vec{v})$ and the probability of the survival of the H^- ion as it leaves the target $f(\vec{v})$. The H^- yield is then given by

$$H^- \text{yield} = \frac{1}{N_i} \int_v n(\vec{v}) P_-(\vec{v}) f(\vec{v}) d\vec{v}. \qquad (1)$$

If, for the sake of discussion, we assume that the terms are separable,

$$H^- \text{yield} = R_N f P_- \qquad (2)$$

where,

R_N is the total particle reflection coefficient

f is the (averaged) probability of H^- survival

P_- is the (averaged) probability of H^- formation.

To discuss the H^- yield measurements in terms of equation (2), we need to know the dependence R_N, f, P_- on the incident energy. Hiskes has shown that calculated values of R_N for alkali-metals are a monotonically decreasing function of the incident energy, in the energy range of these measurements.[19]

In the accompanying paper,[20] Hiskes and Schneider show that P_- is a monotonically decreasing function of the average perpendicular exit velocity, $\langle v_\perp \rangle$, which increases with increasing incident velocity. Similarly, f is a monotonically increasing function of the incident velocity. Therefore, the fact that all the H^- and D^- curves have a maxima at incident energies above 200 eV indicates that the survival probability is the major factor in determining the negative ion yield at incident energies below a few hundred electron volts. Similarly, at high incident energies, the probability of formation and reflection are the factors determining the H^-, D^- yields. Features (2) and (3) above, can be explained by the fact that at the same incident energy the

reflection probability decreases in the order given in (2) and that the work function increases in the same order: The lower the work function, the larger the survival probability at lower incident energies, thus shifting the H^-, D^- yield maximum to lower incident energy.

The isotope effect (4), and (5) arises from the fact that R_N, f, and P_- have different energy dependences. R_N is almost the same for H and D at the same incident energy. However, the incident velocity and the average reflected velocity are higher for H than for D. Thus, at low incident energies, where survival probability dominates, H^- has a higher survival probability and hence a higher yield than D^-. On the other hand, at high incident energies, where formation probability dominates, D^- has a higher formation probability, and thus a higher yield than H^-. This argument also explains the crossing over of the H^- and D^- yield curves. The fact that the isotope effect becomes more pronounced as the target mass and atomic number become smaller is probably due to the mass difference between H and D (1 a.m.u.) becoming more significant compared to the target mass (133 a.m.u. for Cs to 7 a.m.u. for Li), thus giving rise to different velocity distributions of H^- and D^- leaving the target.

B. Thin Coverage

The thin-coverage measurements were made using cesium on a Ni substrate. This combination of materials was chosen because of the low value of the minimum work function (1.6 eV)[21] which can be obtained at a fractional Cs monolayer coverage of the Ni surface, and because Ni was a convenient material to work with. In figure 14, we show the change in the surface work function and the backscattered D^- yield as the Cs

coverage is increased on a Ni substrate which was cleaned by abrasion before being installed in the vacuum chamber. The substrate was heated to about 1400K, hot enough to deposit a clearly visible Ni layer on the facing collector plate in about 30 minutes, at a background pressure of 10^{-9} Torr, and was allowed to cool to room temperature over night at a background pressure of 4×10^{-10} Torr before the Cs was evaporated. It can be seen in Figure 14 that the maximum in the backscattered D^- yield occurs at the Cs coverage that produces the minimum work function, for both 170 and 550 eV/d incident energies. The maximum D^- yield of 0.14 for thin coverage is almost twice as high as the maximum of 0.08 for thick Cs (see Figure 5). The variation of the backscattered D^- yield with incident energy, as the Cs coverage is increased on a Ni substrate, is illustrated in Figure 15. The backscattered D^- yield curves show a definite change in energy dependence as the Cs coverage is increased: At low Cs coverages the D^- yield decreases as the energy decreases, at optimum Cs coverage (evaporation no. 9) the D^- yield increases with decreasing energy, and at thicker coverage (evaporation no. 11) the D^- yield again decreases with decreasing energy. This change in the energy dependence may be explained by a hypothesis presented by Hiskes and Karo[7] and D^- yields from W with a partial monolayer of Cs coverage: At partial monolayer coverages, near the minimum in the work function, an electric dipole layer is produced at the Cs--substrate interface, which greatly enhances the probability of survival of the D^-. As discussed in the preceding section, the probability of survival dominates the backscattered D^- yield for incident energies below a few hundred eV, so that any change in the survival probability

should be apparent in the D^- yield. For higher incident energies, the D^- yield depends more upon the probability of formation than survival, so that the effect of the dipole layer will not be as pronounced.

A quantitative discussion of these results is presented in the accompanying paper by Hiskes and Schneider.[20]

We gratefully acknowledge H. A. Hughes, L. A. Biagi, and the members of their mechanical shops. Also C. M. Garrett for maintenance of the electronics associated with the experiment.

References

1. K. N. Leung and K. W. Ehlers, Abstracts of the IEEE International Conference on Plasma Science, (Montreal, 1979), pp. 32.
2. R. Middleton, IEEE Trans. Nucl. Sci., 23, 1098 (1976).
3. Yu. I. Belchenko, G. I. Dimov and V. G. Dudnikov, Izv. Akad. Nauk. SSSR Ser. Fiz., 37, 2573 (1973).
4. Yu. I. Belchenko, G. I. Dimov and V. G. Dudnikov, Zh. Tekh. Fiz., 45, 68 (1973) [Sov. Phys. - Tech. Phys., 20, 40 (1975)].
5. G. I. Dimov, presented at the Second Symposium on Ion Sources and Formation of Ion Beams, Berkeley, California, 1974.
6. J. R. Hiskes, A. Karo and M. Gardner, J. Appl. Phys., 47, 3888 (1976).
7. J. R. Hiskes, A. Karo, Proc. of the Symposium on Production and Neutralization of Negative Hydrogen Ions and Beams, Brookhaven 1977, pp. 63-69, (LBL Report 6839).
8. M. E. Kishinevskii, Institute of Nuclear Physics (Novosibirsk) Report IYAF 76-18 (1976).
9. O. S. Oen and M. T. Robinson, Nucl. Inst. and Methods, 132, 647 (1976).
10. W. Eckstein, H. Verbeek and S. Datz, Appl. Phys. Lett., 27, 10, pp. 527-528 (1975).
11. W. Heiland, U. Beitat and E. Taglaner, Phys. Rev. B, 19, 4, pp. 1677-81 (1979).
12. P. J. Schneider, "Negative Ion Production by Backscattering from Alkali-Metal Surfaces Bombarded by Ions of Hydrogen and Deuterium," Ph.D. Thesis, Univ. of California, Berkeley, 1980, LBL Report 10616.

13. P. Meischnder and H. Verbeek, Max Planck Institute for Plasma Physics (Garching, W. Germany), Report IPP 9/18 (1975).

14. W. Eckstein, P. Matschke and H. Verbeek, Proc. Sec. Conf. on Surface Effects in Controlled Fusion Devices, San Francisco, California (1976) (North Holland Publishing Co., Amsterdam, 1976).

15. J. R. Hiskes, private communication of results from the Marlowe Code[9].

16. P. A. Anderson, Phys. Rev., 47, 958 (1935).

17. C. Herring and M. H. Nichols, Rev. Mod. Phys., 21, 185 (1949).

18. J. Millman and S. Seely, Electronics (McGraw Hill, New York, 1955), pp. 107.

19. J. R. Hiskes, XIV International Conference on Phenomena in Ionized Gases, Grenoble, France 1979.

20. J. R. Hiskes and P. J. Schneider submitted to

21. C. A. Papageorgopoulos and J. M. Chen, Surf. Sci., 52, pp. 40-52, (1975).

Figure Captions

Figure 1. Line drawing of the apparatus within the experimental chamber, which was used to measure the Negative Ion Secondary Emission Coefficient (NISEC).

Figure 2. Apparent NISEC vs. the magnitude of the applied magnetic field for the case of 6 keV/d D_3^+ on an untreated Mo target. The target bias was -6 kV, resulting in an electric field of 4.6 kV/cm.

Figure 3. Mass spectra of positive ions sputtered by 8 keV Ar^+ incident upon (a) an untreated Cu target and (b) the same Cu target with thick Na coverage.

Figure 4. Backscattered H^- yield vs incident energy for H_2^+--o and H_3^+--o incident on thick Cs (work function, ϕ_w = 1.9 eV).

Figure 5. Backscattered D^- yield vs incident energy for D_2^+--o and D_3^+--o incident on thick Cs (work function, Cs (ϕ_w = 1.9 eV).

Figure 6. Backscattered H^- yield vs incident energy for H_2^+--o and H_3^+--o incident on thick Rb (ϕ_w = 2.08 eV).

Figure 7. Backscattered D^- yield vs incident energy for D_2^+--o and D_3^+--o incident on thick Rb (ϕ_w = 2.08 eV).

Figure 8. Backscattered H^- yield vs incident energy for H_2^+--o and H_3^+--o incident on thick K (ϕ_w = 2.24 eV).

Figure 9. Backscattered D^- yield vs incident energy for D_2^+--o and D_3^+--o incident on thick K (ϕ_w = 2.24 eV).

Figure 10. Backscattered H^- yield vs incident energy for H_2^+--o and H_3^+--o incident on thick Na (ϕ_w = 2.28 eV).

Figure 11. Backscattered D^- yield vs incident energy for D_2^+--o and D_3^+--o incident on thick Na (ϕ_w = 2.28 eV).

Figure 12. Backscattered H^- yield vs incident energy for H_2^+--o and H_3^+--o incident on thick Li (ϕ_w = 2.49).

Figure 13. Backscattered D^- yield vs incident energy for D_2^+--o and D_3^+--o incident on thick Li (ϕ_w = 2.49).

Figure 14. Backscattered D^- yield and change in surface work function vs evaporation number for Cs deposited on a room temperature Ni substrate: Δ, change in work function; O, 170 eV/d D_3^+ incident; O, 550 eV/d D_3^+ incident.

Figure 15. Variation of the backscattered D^- yield with incident energy as the Cs coverage is increased on a Ni substrate. The numbers to the right of the curves denote the change in the surface work function and those on the left indicate the evaporation number. The Cs thickness increases with evaporation number. The solid circles indicate Cs thickness beyond optimum coverage.

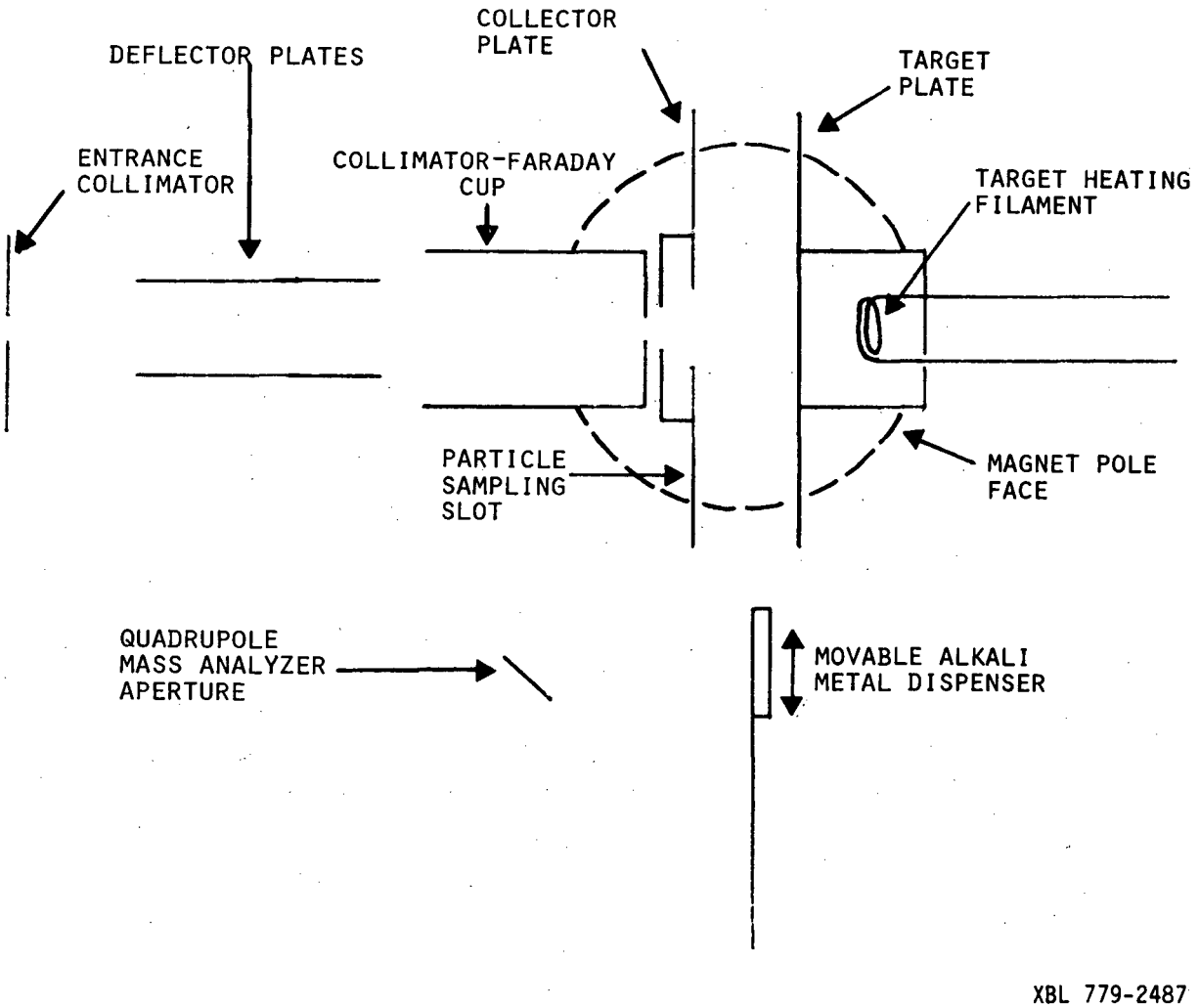
COLLECTOR PLATE
DEFLECTOR PLATES
TARGET PLATE
ENTRANCE COLLIMATOR
COLLIMATOR-FARADAY CUP
TARGET HEATING FILAMENT
PARTICLE SAMPLING SLOT
MAGNET POLE FACE
QUADRUPOLE MASS ANALYZER APERTURE
MOVABLE ALKALI METAL DISPENSER
XBL 779-2487

Fig. 1

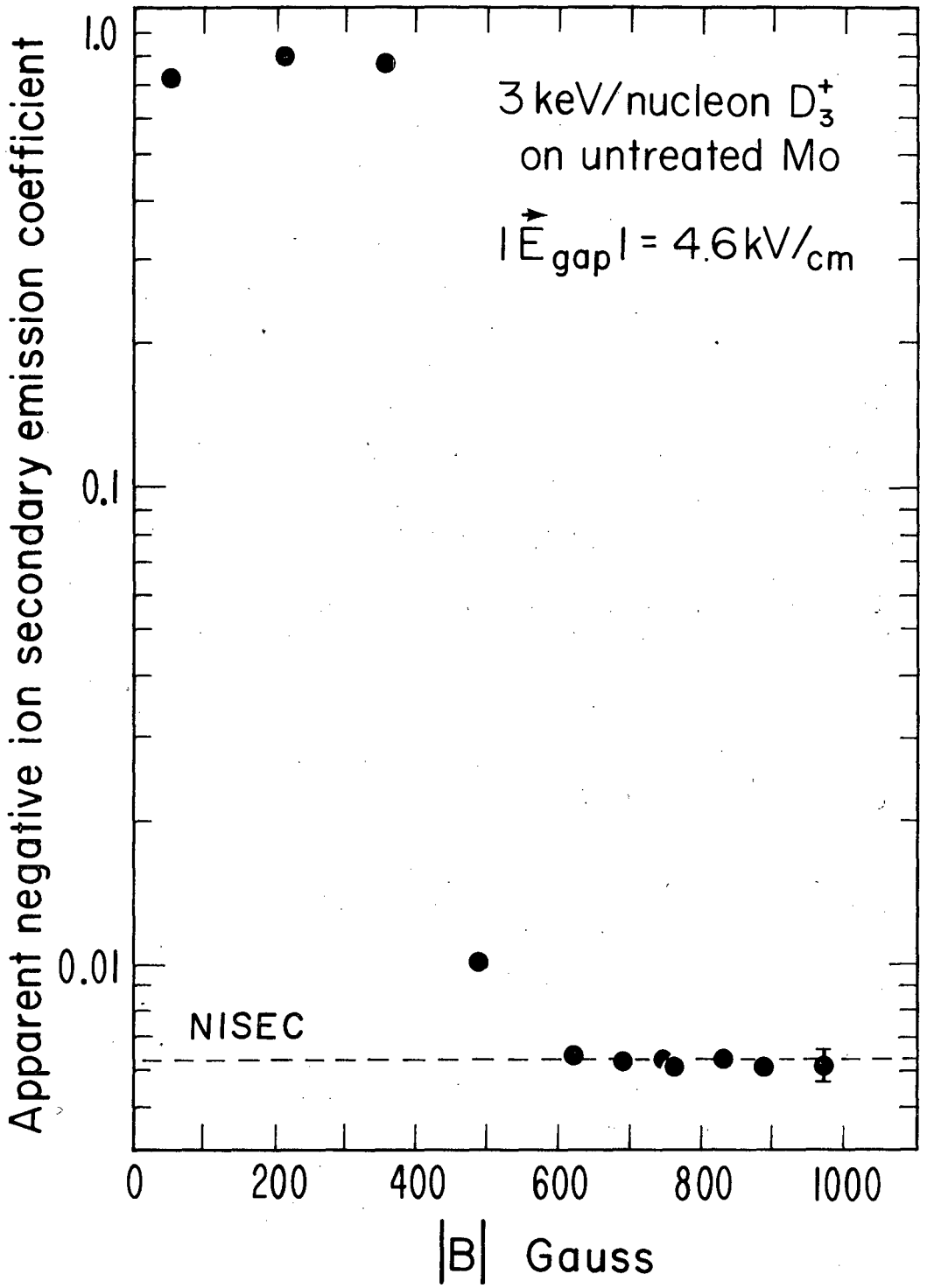

XBL 779-1934

Fig. 2

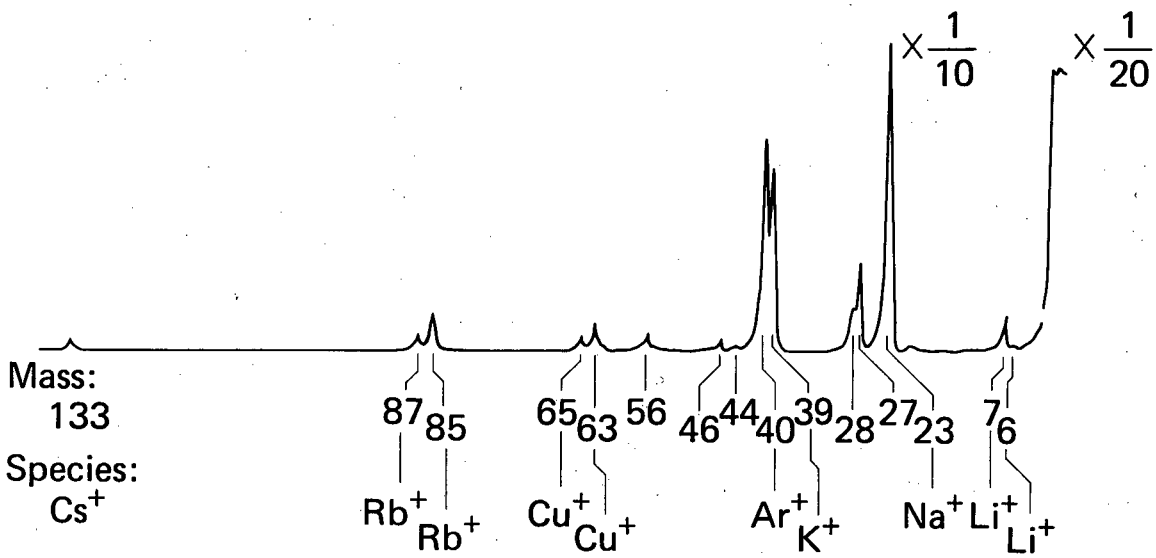

Positive ions sputtered from an untreated Cu target bombarded by 8 keV Ar^+.

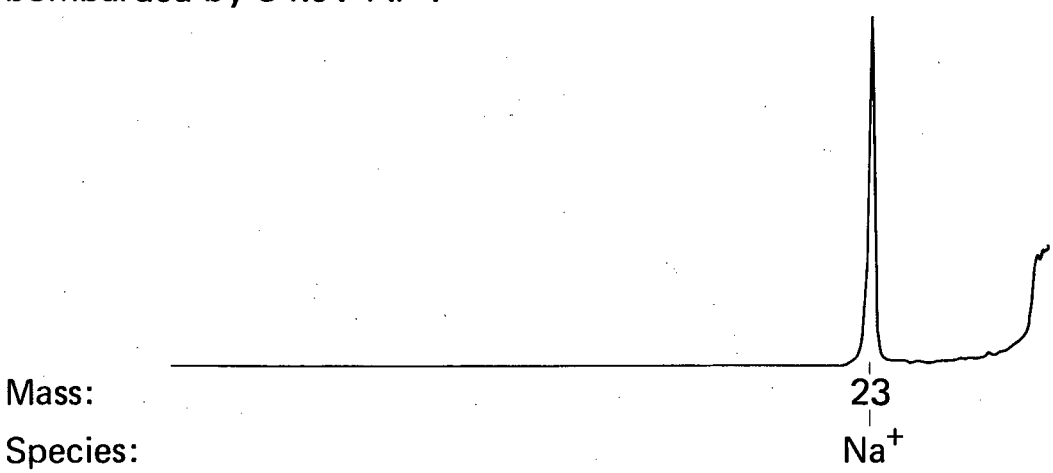

Positive ions sputtered from a freshly evaporated Na surface bombarded by 8 keV Ar^+.

XBL 806-10349

Fig. 3

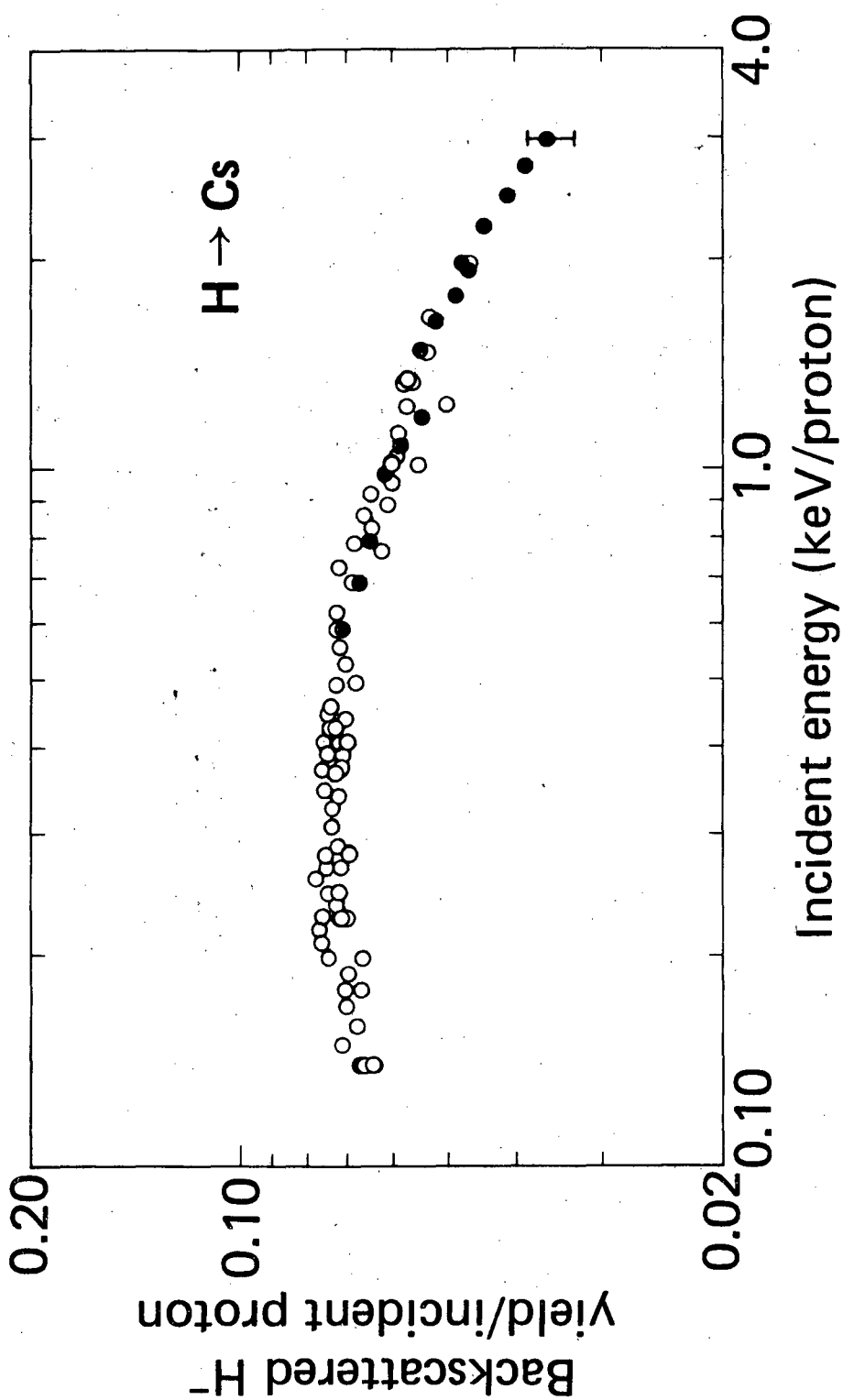

XBL 806-10358

Fig. 4

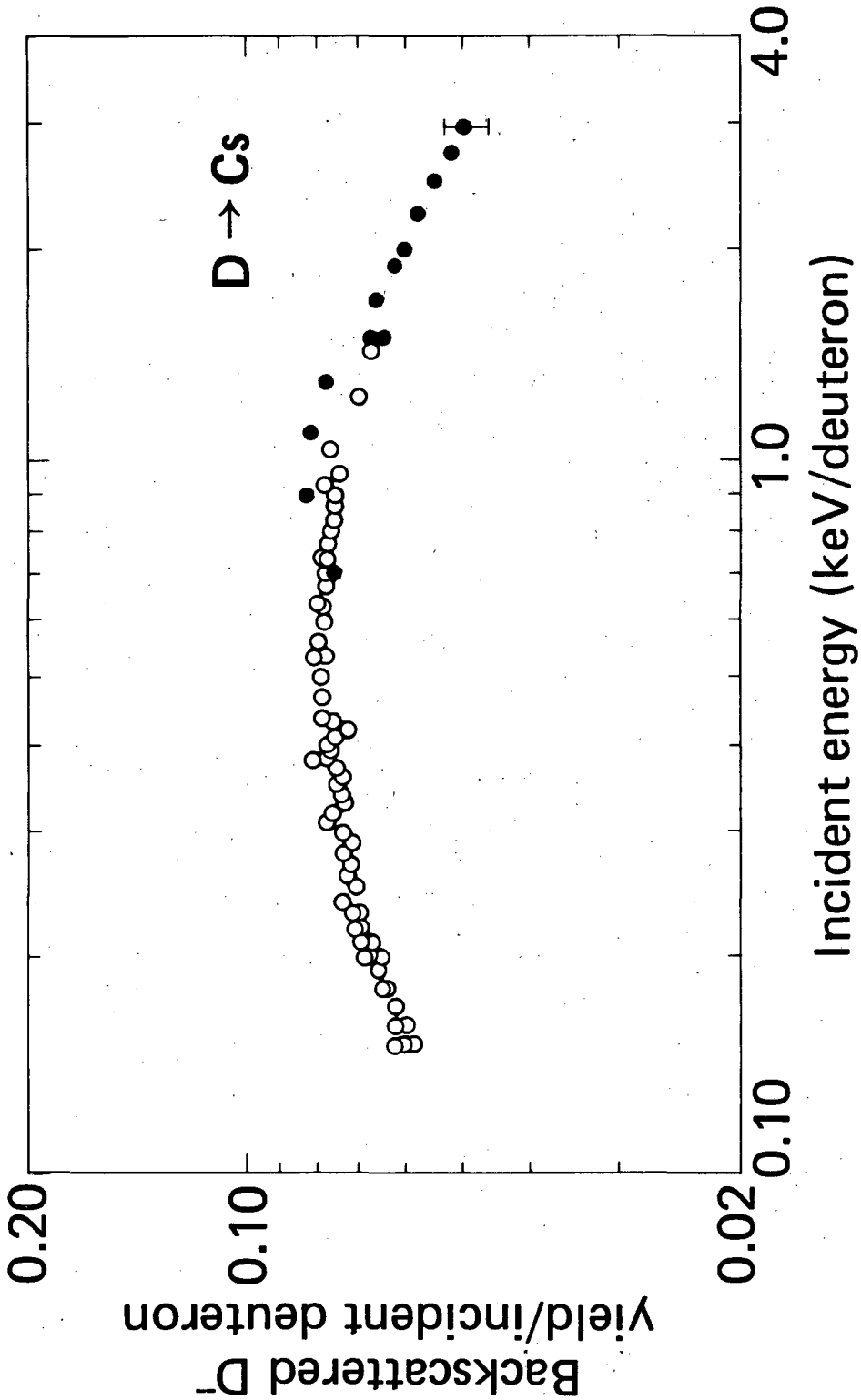

XBL 806-10359

Fig. 5

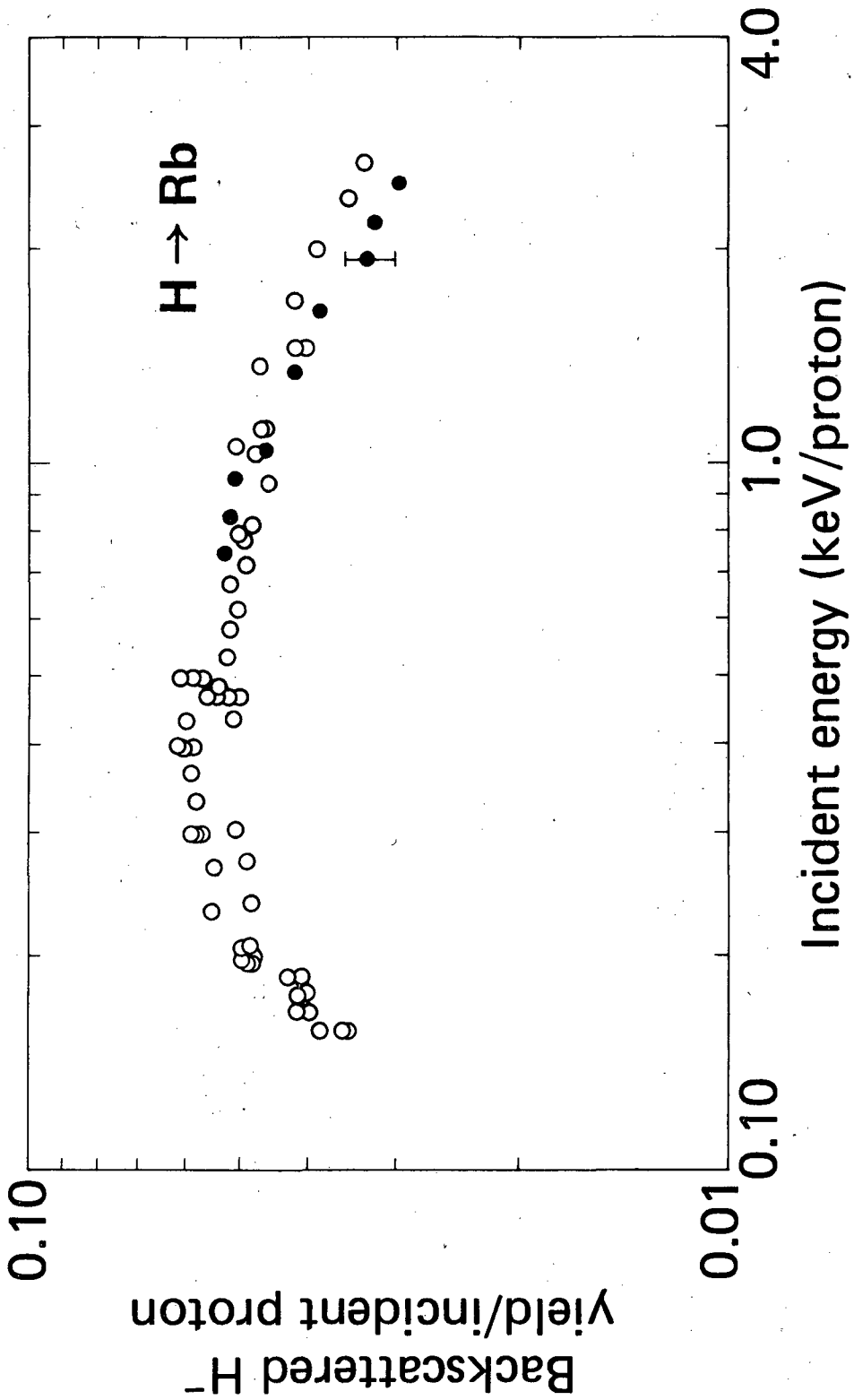

XBL 806-10352

Fig. 6

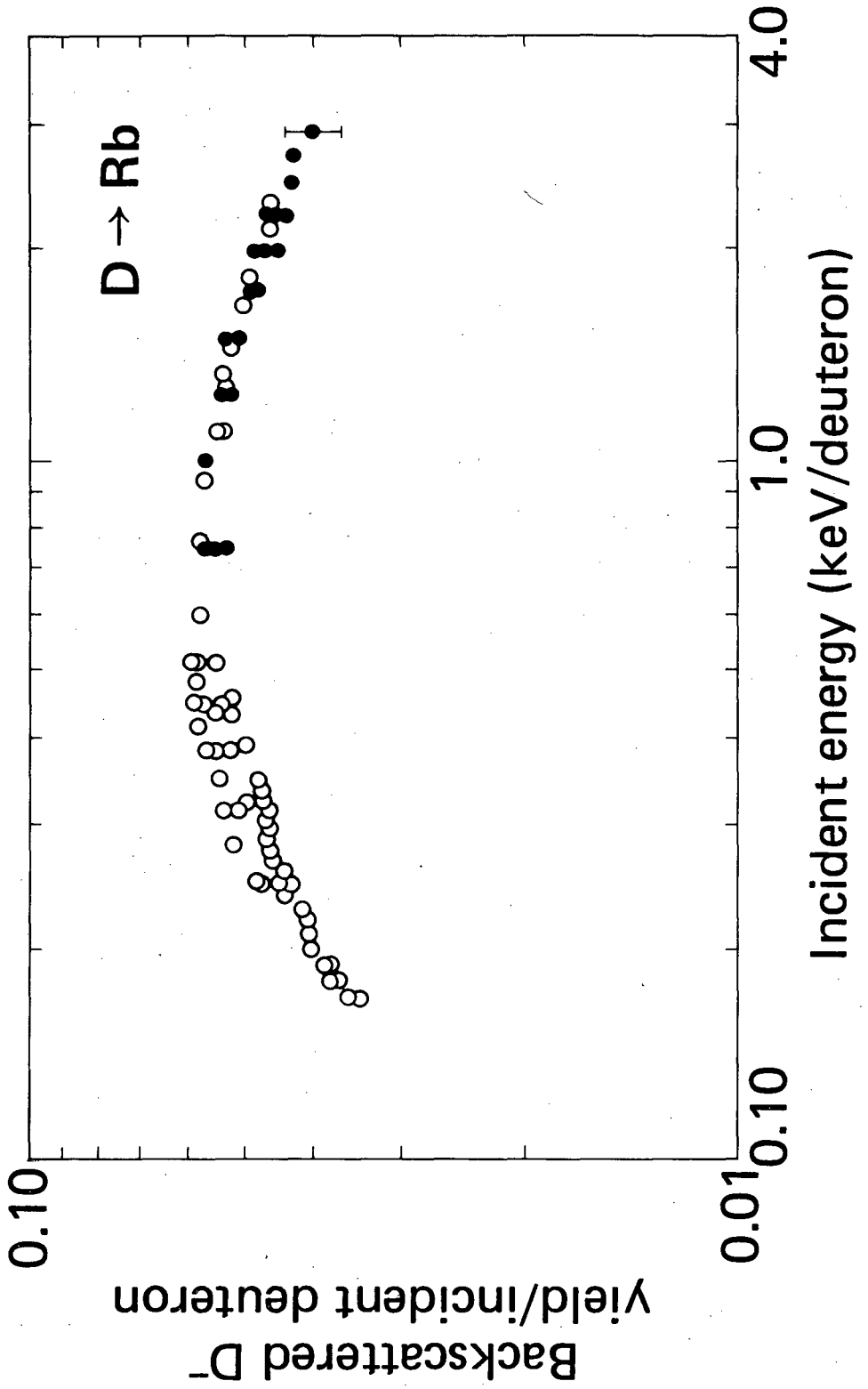

XBL 806-10354

Fig. 7

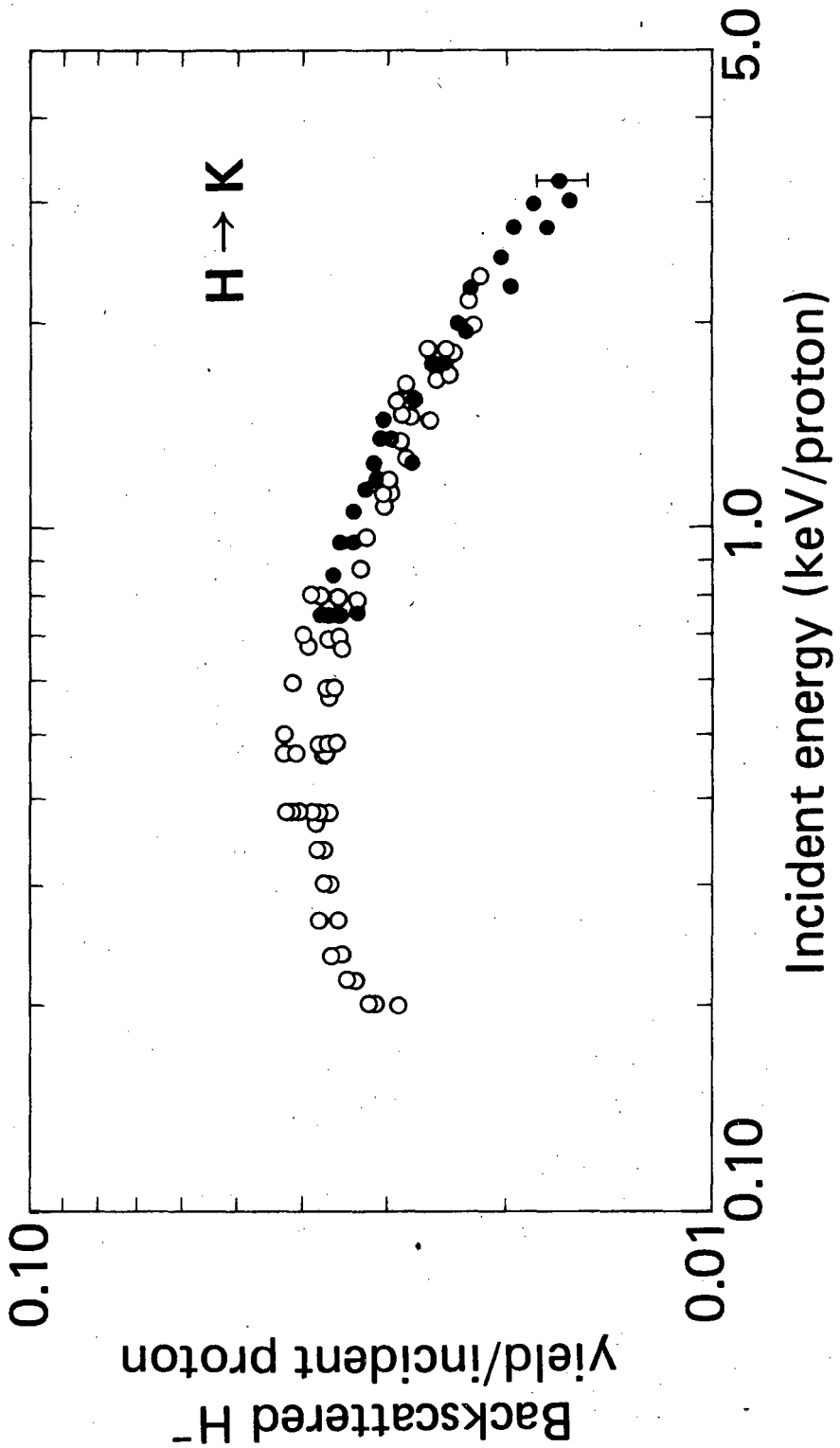

XBL 806-10355

Fig. 8

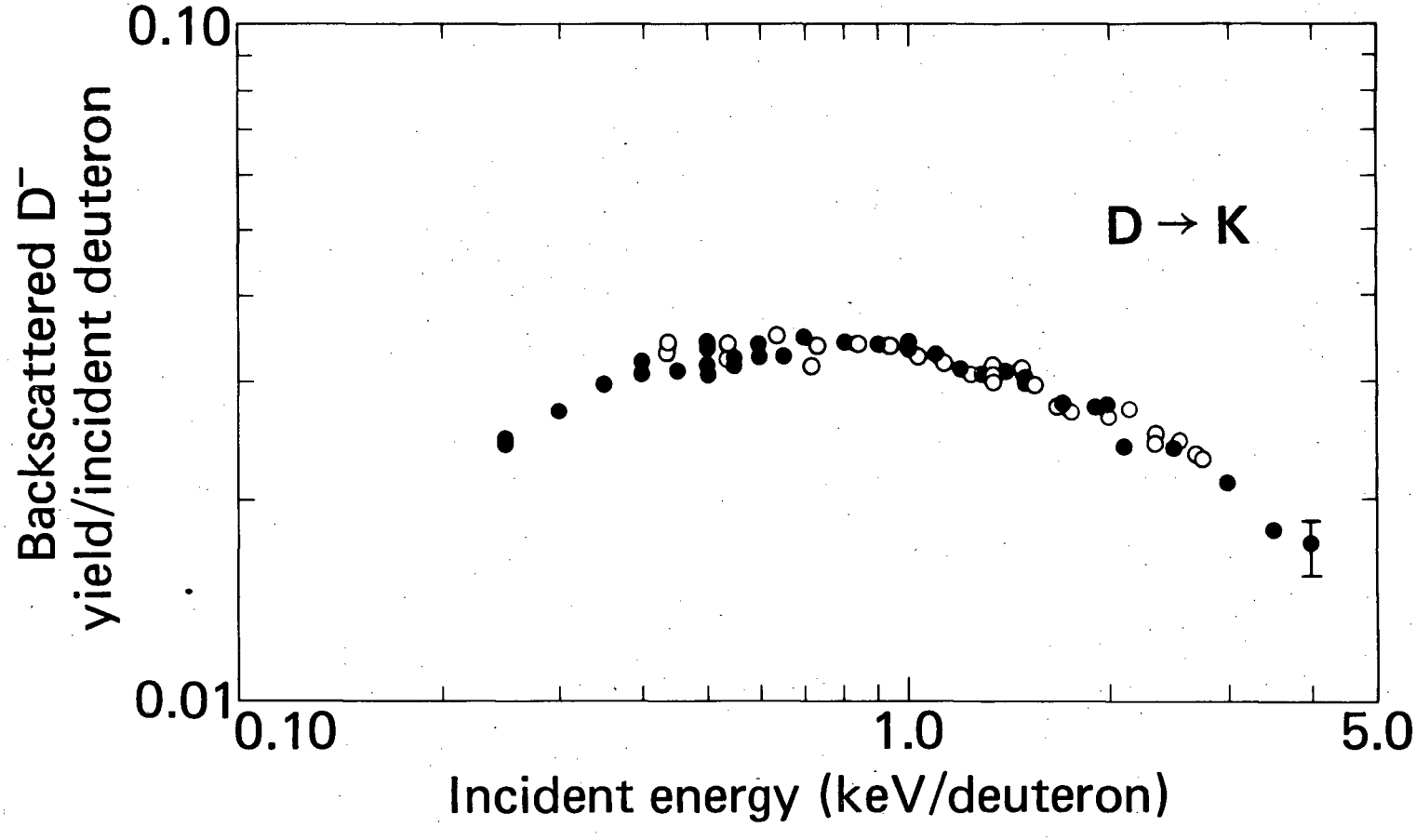

XBL 806-10360

Fig. 9

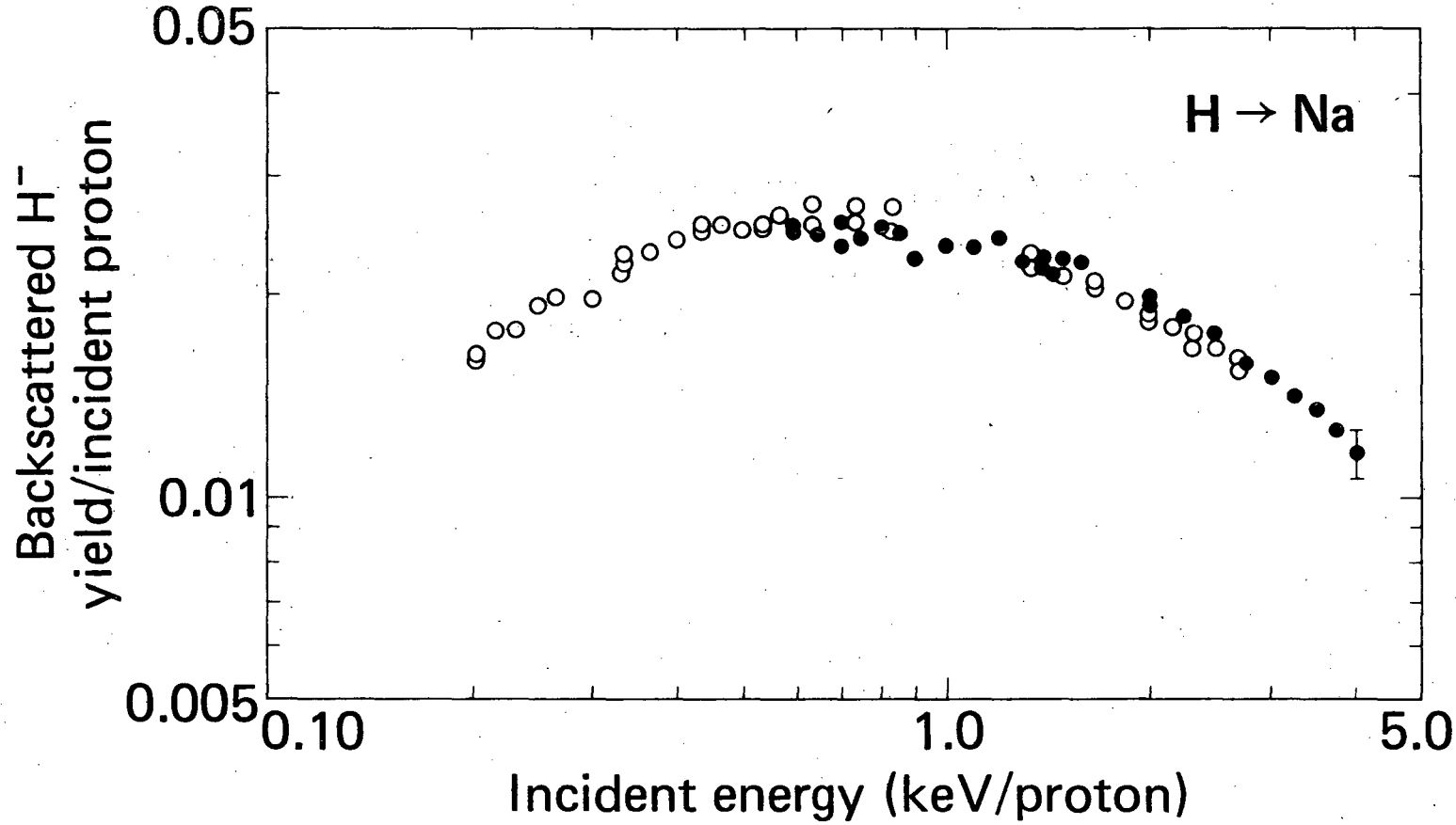

XBL 806-10353

Fig. 10

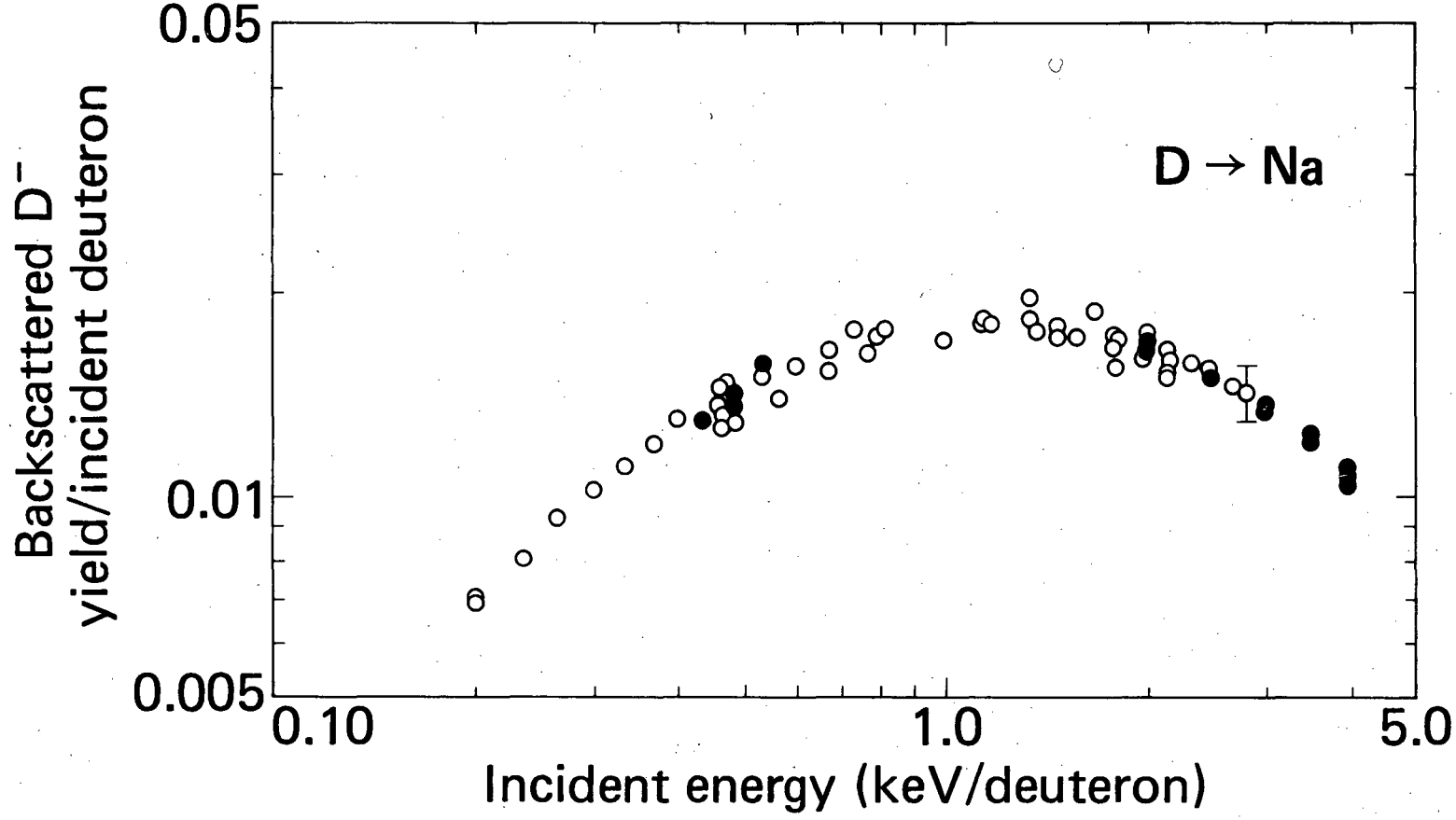

XBL 806-10351

Fig. 11

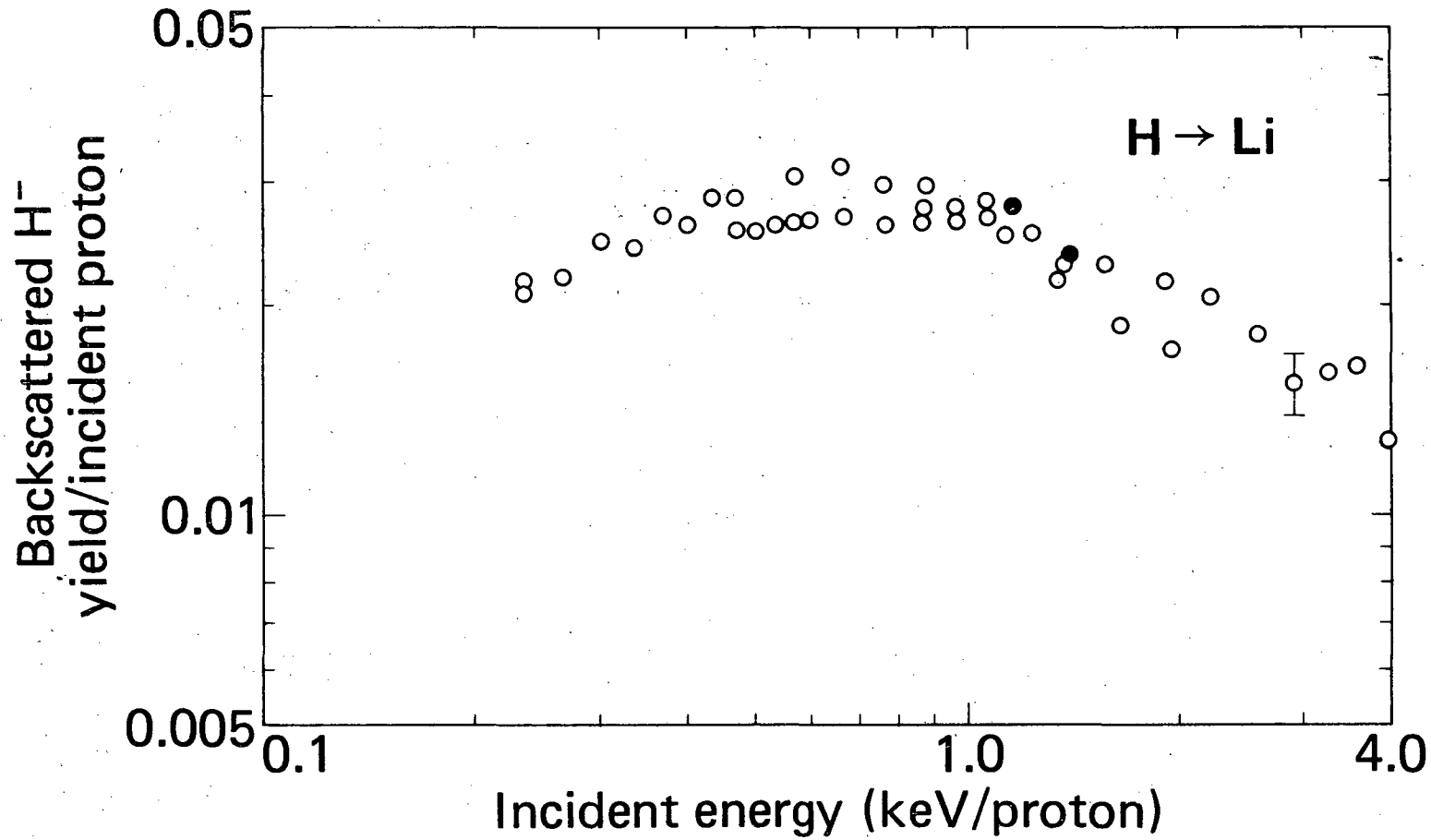

XBL 806-10356

Fig. 12

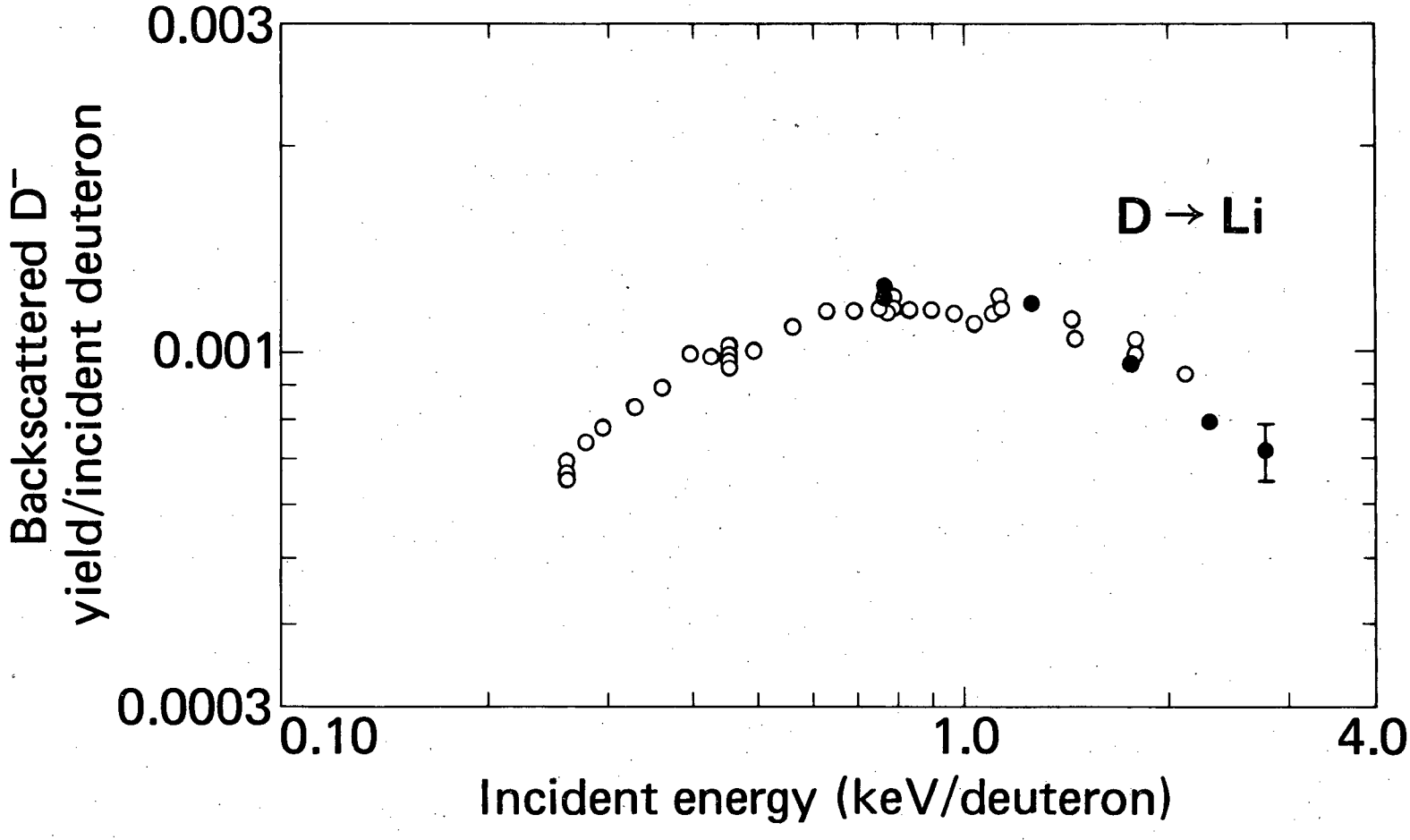

XBL 806-10357

Fig. 13

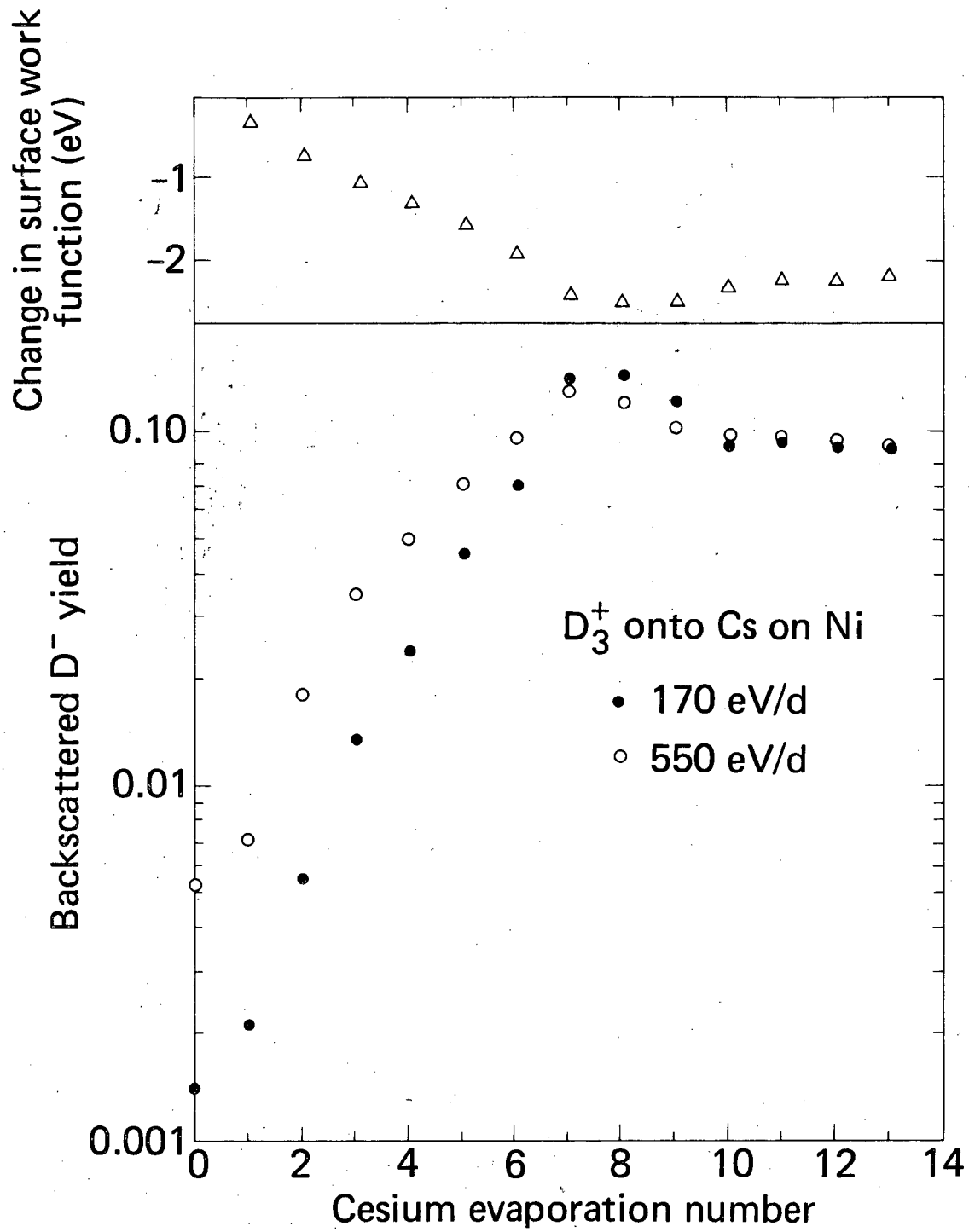

XBL 806-10350

Fig. 14

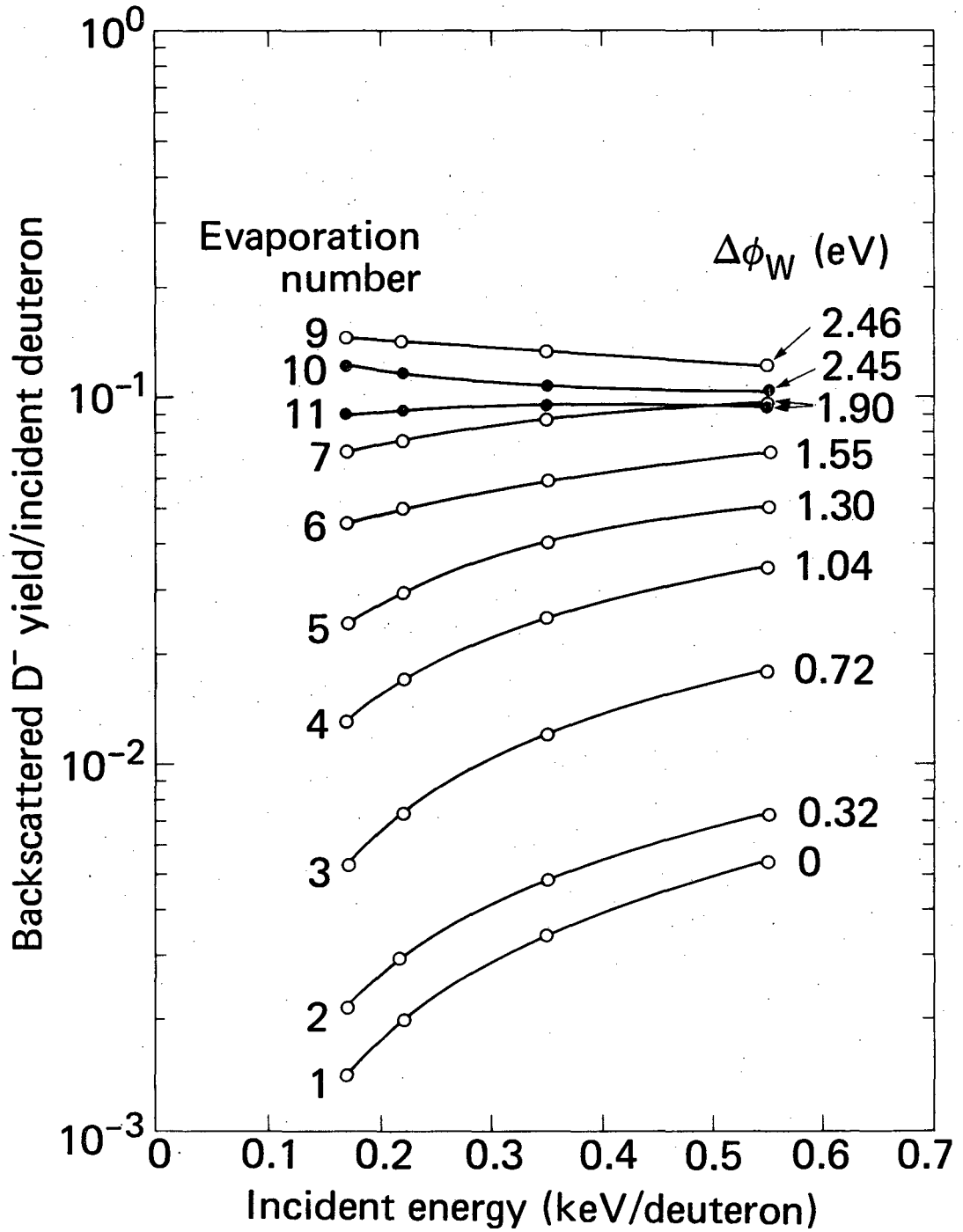

XBL 806-10361

Fig. 15

This report was done with support from the Department of Energy. Any conclusions or opinions expressed in this report represent solely those of the author(s) and not necessarily those of The Regents of the University of California, the Lawrence Berkeley Laboratory or the Department of Energy.

Reference to a company or product name does not imply approval or recommendation of the product by the University of California or the U.S. Department of Energy to the exclusion of others that may be suitable.

TECHNICAL INFORMATION DEPARTMENT
LAWRENCE BERKELEY LABORATORY
UNIVERSITY OF CALIFORNIA
BERKELEY, CALIFORNIA 94720